NURETH14-289

MCCI SIMULATION COMPARISON BETWEEN MELCOR AND CORQUENCH

K. Robb, M. Corradini University of Wisconsin-Madison, WI, U.S.A.

Abstract

This paper presents a comparison between the MELCOR and CORQUENCH codes in modeling the progression of a reactor scale ex-vessel core melt. This study investigates the impact of advanced modeling options on the progression of molten corium-concrete interactions (MCCI). Two cooling phenomena, water ingression and melt eruptions, and the crust anchoring phenomenon were shown to largely impact the accident progression. Recommendations are made concerning updating CONRCON-Mod3 within MELCOR and future research activities.

Introduction

Severe accidents at nuclear power plants, while of very low probability, are of interest due to the possibility of releasing radioactive material into the environment. During one such postulated accident scenario the reactor core melts and exits the pressure vessel. The core debris forms a pool on the concrete basemat of containment. The core debris, continually heated from decay heat and chemical reactions, can reach temperatures above the decomposition temperature of the underlying concrete. During the ex-vessel core melt accident scenario, the containment structure is the last barrier preventing the release of radionuclides into the environment. The ability to determine the rate of concrete ablation and associated gas generation is important to predict the probability and associated timing of containment failure. A number of computer codes have been developed with the ability to model the ex-vessel core melt interaction with concrete.

The CORCON code was developed as a stand alone computer program at Sandia National Laboratories to model molten core-concrete interactions (MCCI), [1]. Based on MCCI experimental work, such as the SWISS [2] and SURC [3] test series, the CORCON code was updated to include a number of modeling enhancements. When released in 1993, CORCON-Mod3 "represent[ed] the current state-of-the-art for simulating core debris interactions with concrete" [4]. CORCON-Mod3 was later integrated into the systems level code MELCOR [5]. MELCOR is one code used by the U.S. Nuclear Regulatory Commission to model and analyze the progression of possible nuclear power plant accidents.

Since the development of CORCON-Mod3, the MACE, MCCI-1, MCCI-2 as well as other international MCCI research programs have been conducted focusing on the impact of an overlying water layer on melt coolability [6]. From these programs, new insight has been gained into many phenomena including: initial transient crusting and concrete ablation [7], crust formation and strength [8], melt eruptions through the top crust after formation [9, 10], and water ingression into the top crust [11]. The CORQUENCH code was developed as part of the

OECD/NEA MCCI-1 and MCCI-2 research programs [7] with a focus on modeling the effects of an overlying water layer. CORQUENCH provides a platform in which new MCCI models and phenomena can be easily integrated and evaluated within the context of a coupled MCCI systems code.

The current work investigates the predictive capabilities of CORCON-Mod3 within the MELCOR systems code (version 1.8.6) and CORQUENCH (version 3.03) with respect to an exvessel core melt scenario under flooded conditions. A base case core melt scenario was constructed based on the characteristics of the Zion Nuclear Power Station. Comparisons of the accident progression are made between the MELCOR and CORQUENCH simulations.

The purpose of the comparison is to identify what new modeling options, developed since the last revision of CORCON-Mod3, have a large impact on accident progression simulations. Differences in modeling between the codes are highlighted and the consequences are illustrated. Based on this work, suggestions are made concerning future research.

1. Base Case Setup

The following sections describe the simulation initial conditions and code modeling options used. The initial and boundary conditions are based on the Zion nuclear power station and are described in Section 1.1. The base case modeling options used in MELCOR and CORQUENCH are described in Section 1.2. The base case modeling options for the two codes were chosen to be similar to see if there is reasonable agreement between the codes. Later, in Section 2.0, the modeling options are varied to illustrate the impact of the models on the predicted accident progression.

1.1 Initial and Boundary Conditions

The Zion Nuclear Power Station, located in Lake County, IL, USA, consisted of two Westinghouse 4-loop PWR's. Power operations at both units ceased in 1998. The postulated scenario models the relocation of 75% of the reactor materials with an initial temperature of 3000 K. The melt is representative of the relocation of 75% of the available in-core steel, Zr, and UO₂, 56% of the lower core structure and 7.5% of the RPV lower head. The melt composition is given in Table 1. The Zion plant dry-well is a rectilinear key way geometry which is modeled as a cylindrical cavity with a 4.67 m radius. The large spreading area (68.5 m²) results in an initial collapsed melt height of approximately 24 cm. The core debris is modeled to instantly arrive and spread uniformly over the dry concrete basemat 2 hours after reactor shutdown. This delay only impacts the starting point on the decay heat curve. The decay heat within the melt is modeled with a 12 point approximation in both codes, Table 3. The Zion plant concrete type is limestonecommon sand with a composition given in Table 2. The concrete solidus, liquidus, and decomposition temperature were set to 1393 K, 1568 K, and 1500 K, respectively. Water is assumed to be introduced on top of the melt 30 minutes after the melt arrives at the basemat (2.5 hours after reactor shutdown). The 1m water layer is maintained over the melt at the saturation temperature throughout the remaining simulation. The containment pressure was held constant at

1 atm. The simulation ends when either 5 days time has passed (from melt relocation time) or the melt quenches.

Table 1 Relocated Core Debris Composition

Melt	Weight %	Mass
Constituent	[%]	[kg]
UO_2	58.0	73500
Zr	3.0	3750
ZrO_2	12.0	15190
Fe	20.3	25760
Cr	4.6	5840
Ni	2.2	2748
Total Mass [l	126788	
Approx. Volu	16.6	
Approx. Heig	24.2	

^{*}Initial Melt Density ~7635 kg/m³ (collapsed, no gas void)

Table 2 Concrete Composition

Concrete	Weight %
Constituent	[%]
SiO ₂	38.30
CaO	24.10
CO_2	20.40
MgO	8.30
H ₂ O (evap)	4.20
H ₂ O (bound)	2.00
$A1_2O_3$	1.70
Fe ₂ O ₃	0.80
K_20	0.10
Na ₂ O	0.06
TiO ₂	0.04

1.2 Base Case Modeling Description

The following summarizes the main base case modeling options used in each code. Additional code descriptions, default parameters, and material property routines are found in the code reference manuals [4, 5, 7]. In CORQUENCH, the melt eruption, water ingression, and crust anchoring options are disabled. The MELCOR-CORCON module lacks models for any of these phenomena. Both codes contain a full boiling curve for the upward heat transfer when an overlying water layer is present. The emissivity of the melt pool is determined by a subroutine in COROUENCH and was found to be around 0.7 during the first couple hours of simulated time. The user must specify the melt emissivity in MELCOR and it was set to 0.7. The concrete cavity emissivity was specified as 0.6 for both codes. In both codes, subroutines were used to determine the thermal conductivity of the melt as a function of melt composition. While MELCOR can model a melt pool with segregated layers, the melt was modeled as a homogeneous pool in both MELCOR and CORQUENCH. Both codes use the slag film model for the melt/concrete interfacial heat transfer and the quasi-steady concrete ablation model. MELCOR has a sophisticated cavity geometry tracking model whereas CORQUENCH maintains a right cylindrical geometry. The initial cavity profile declaration in MELCOR used 60 nodes (30 bottom, 5 fillet, 25 sidewall) with the ray origin set 1m up from the basemat. CORQUENCH determines the oxidation of Zr, Cr, and Fe by H₂O and CO₂ based on a hierarchy with oxidation of Zr first, Cr second, and Fe last [7]. The option for the condensed phase reaction between Zr and SiO₂ was enabled which proceeds in parallel with Zr oxidation from H₂O and CO₂. MELCOR contains many possible melt constituents and determines chemical reactions through minimizing the Gibbs free energy of a metallic, oxidic, and gaseous phase, each of which is treated as ideal solutions [5, 4]. The maximum time step for MELCOR's adaptive time step routine was set to 1 s. A constant time step of 0.05 s was used in CORQUENCH.

1.3 Base Case Code Comparison

The accident progression predicted by MELCOR and CORQUENCH for the base case settings are quite similar. For all comparisons, time zero is when the melt relocates onto the concrete containment floor. The figures have been scaled to show the long term accident progression.

The axial and radial ablation distance is plotted as a function of time in Figure 1. MELCOR and CORQUENCH predicted continued concrete ablation after the 5 days of simulation time. CORQUENCH uses the same heat transfer models for the axial and radial concrete surfaces; therefore, the axial and radial ablations are equal. The ablation predicted by CORQUENCH is bound by the axial and radial ablation predicted by MELCOR. The concrete ablation profiles are plotted in Figure 8. Despite differences in the cavity profile tracking, the upper surface area of the melt pool is similar between MELCOR and CORQUENCH, Figure 3.

After water addition the predicted total upward heat transfer and upward heat flux is lower in MELCOR than in CORQUENCH, Figures 2 & 3. Both codes predict long term boiling in the film boiling regime. The difference in upward heat flux is due to differences between the codes' modeling of the film boiling heat flux.

The predicted melt temperatures were similar with CORQUENCH being slightly higher, 80 K, at the end of the simulation, Figures 4 & 5. The melt solidus temperatures were similar, however, the liquidus temperature predicted by MELCOR was quite lower than that predicted by CORQUENCH.

Figures 6 and 7 display the total gas generation predicted due to the concrete decomposition. CORQUENCH predicts the Zr, Cr, and Fe is fully oxidized within approximately 220 minutes whereas oxidation is completed in 380 minutes in MELCOR. The longer oxidation time and additional moles of CO (17% more) and H₂ (9.5% more) generated in MELCOR is attributed to the more complete treatment of possible chemical reactions.

Table 3: Decay Heat

Time After	Melt Power
Reactor SCRAM	Density
[s]	[W/kg UO ₂]
3.60E+03	5.294E+02
5.00E+03	4.886E+02
7.20E+03	4.463E+02
1.00E+04	4.108E+02
2.50E+04	3.231E+02
5.00E+04	2.666E+02
7.50E+04	2.370E+02
1.00E+05	2.175E+02
2.50E+05	1.622E+02
5.00E+05	1.269E+02
7.50E+05	1.084E+02
1.00E+06	9.633E+01

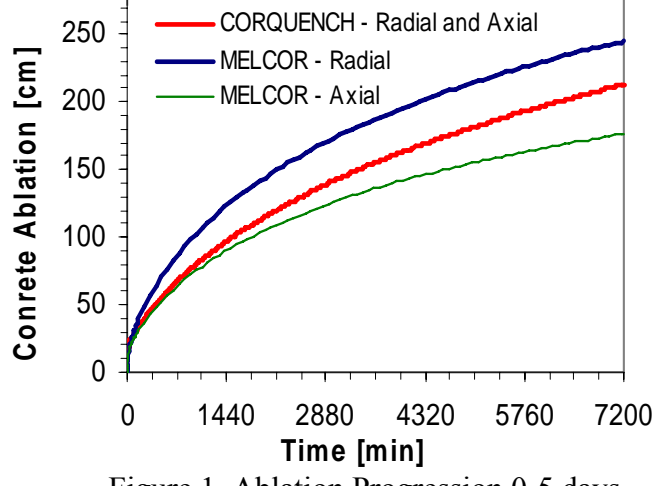


Figure 1 Ablation Progression 0-5 days

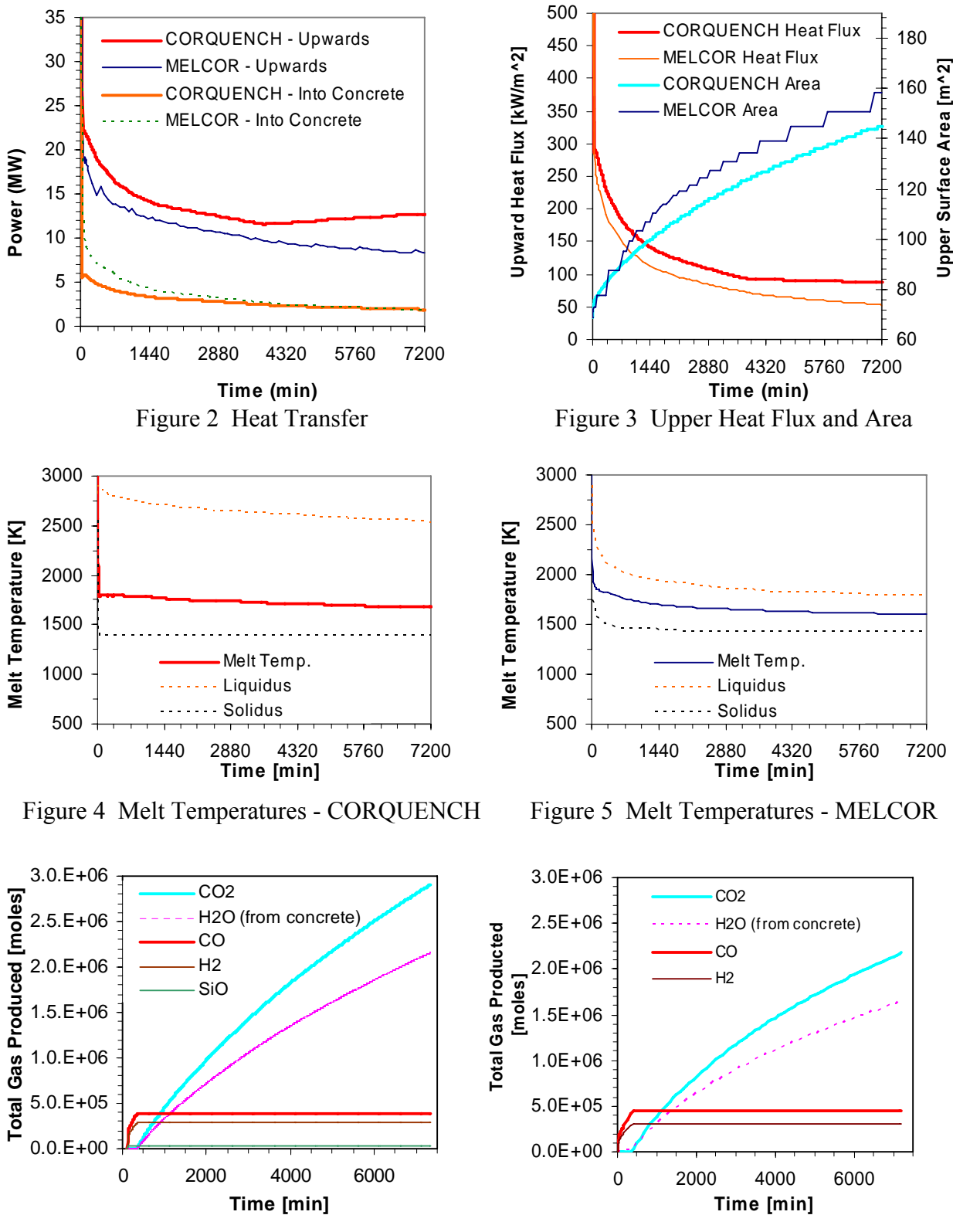


Figure 6 Gas Generation - CORQUENCH Figure 7 Gas Generation - MELCOR

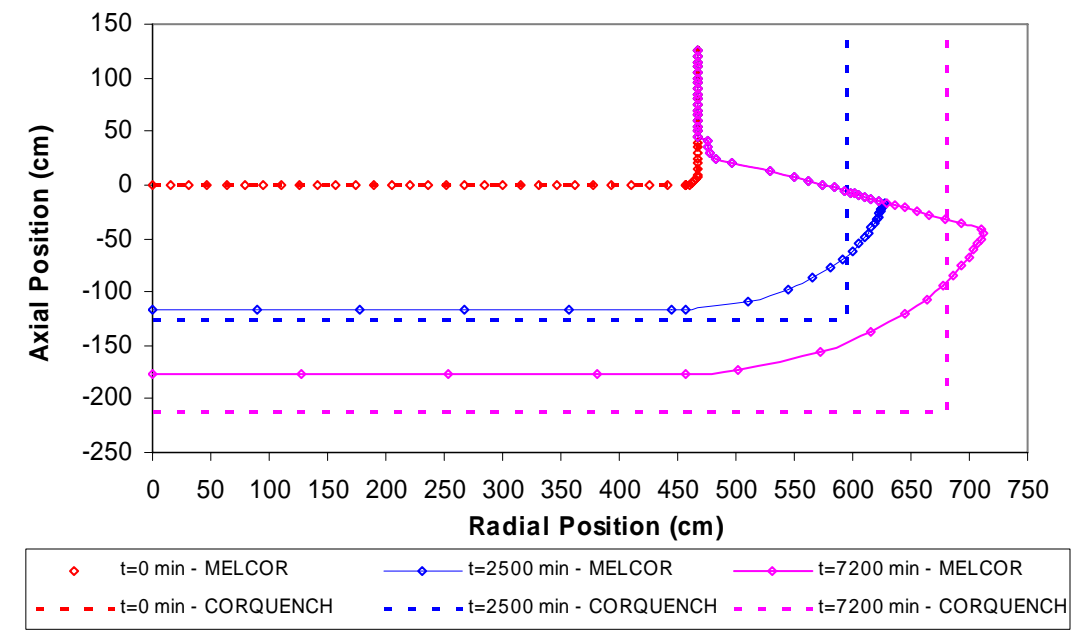


Figure 8 Concrete Ablation Profiles

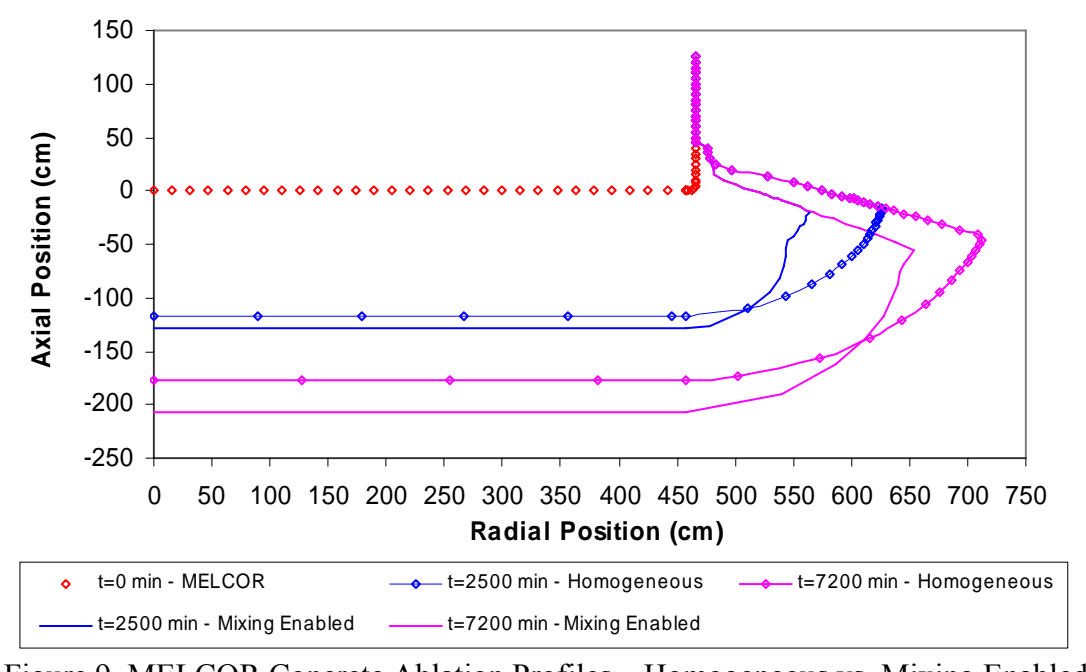


Figure 9 MELCOR Concrete Ablation Profiles – Homogeneous vs. Mixing Enabled

2.0 Modeling Option Variations

The base case modeling options were varied to investigate their impact on accident progression. Table 4 summarizes the modeling option changes and their resulting impact on concrete ablation, melt coolability, total steam and hydrogen produced. As shown, including melt eruptions or water ingression into the crust has a large impact on melt coolability. The melt pool

configuration (homogeneous vs. mixing), crust anchoring, ablation model, and early film boiling break down, had limited impact on melt progression. The following sections investigate these phenomena in more detail.

Table 4: Summary of Modeling Option Variation Results

Code	Section	Modeling Changes (see key)	Quenched or Not Quenched at end of Sim.	Ablation Rate at 5 days [cm/hr]	Ablation Depth at 5 days [cm]	H ₂ Gas Released by end of Sim. [kg]	Total Steam Released by end of Sim. [ton]
	1.3	None	Not Quenched	0.76	213	578	2582
H	2.1	1	Not Quenched	0.74	210	573	2495
Ş	2.4	1,2	Not Quenched	0.74	210	573	2495
	2.5	1,3	Not Quenched	0.70	199	591	2480
CORQUENCH	2.3	1,4	Not Quenched	0.023	58.5	502	3030
OR	2.2	1,5	Quenched	0.00	53.4	552	594
S	-	1,4,5	Quenched	0.00	51.7	546	572
	-	1-5	Quenched	0.00	43.8	564	528
_ ~	1.3	None	Not Quenched	0.51 Ax.	177 Ax.	628	
[0]				0.80 Rad.	245 Rad.		Not Avail.
MELCOR	2.6	6	Not Quenched	0.66 Ax. 0.80 Rad.	206 Ax. 187 Rad	629	

Modeling Changes Key:

None = base case results (see Section 1.0)

- 1 = Early film boiling breakdown enabled (instead of full film boiling curve)
- 2 = Crust anchoring allowed 3MPa crust strength (instead of off)
- 3 = Quasi steady ablation model used (instead of steady ablation model)
- 4 = Melt eruptions enabled ANL model (instead of off)
- 5 = Water ingression enabled Epstein/Lister modeling (instead of off)
- 6 = Evaluate mixing/stratification of melt pool enabled (instead of homogenous)

2.1 Film Boiling Breakdown

After water addition, both the MELCOR and CORQUENCH base cases remained in the film boiling regime throughout the duration of the simulations. Long periods of film boiling, once a crust is present, is not consistent with visual and thermocouple data from MCCI experiments, [7 (section 2.5.2)]. The data suggests the crust is near the saturation temperature [7]. Another investigation into film boiling using a number of different surfaces found film boiling readily breaks down for porous UO₂ and ZrO₂ surfaces [12].

CORQUENCH contains a basic parametric model which is used to cause an early transition from film to nucleate boiling, Eqn 1. When the film boiling heat flux, $q_{fb}^{"}$ (calculated by code), falls below a multiple, $C_{fb,chf}$ (user defined), of the calculated critical heat flux, $q_{chf}^{"}$ (calculated by code), then the boiling regime transitions to nucleate boiling. The code manual provides more detailed descriptions of the implemented boiling models [7].

$$q_{fb}^{"} \stackrel{?}{<} C_{fb,chf} \cdot q_{chf}^{"} \tag{1}$$

In the base case $C_{fb,chf}$ was set to 0.0 which effectively disables the early film boiling transition, yielding the full pool boiling curve. A value for $C_{fb,chf}$ of 0.5 is recommended and used in the validation portion of the code manual [7]. As seen in Table 4, setting $C_{fb,chf}$ to 0.5 did not result in significant changes to the CORQUENCH predictions. However, the boiling regime did transition to the nucleate boiling resulting in a large drop in the crust surface temperature. The drop in crust surface temperature did allow for a slightly thicker crust to form (20% thicker at end of simulation). For all CORQUENCH simulation work in Section 2, $C_{fb,chf}$ has been set to 0.5.

2.2 Water Ingression

As part of the SSWICS test series within the MCCI-1 research program, water ingression into the top crust was investigated [11]. If the crust is impervious to water, as in the CORCON-Mod3 modeling, the maximum top crust thickness is limited by conduction and is of the order of 10 cm. Water ingression into cracks in the crust serves to augment upward heat transfer and facilitates the formation of thicker crusts. To account for water ingression, Lomperski and Farmer [7, 11] developed a model which has been integrated into CORQUENCH based on the work of Epstein [13]. The model is phenomenologically based but contains a multiplicative constant coefficient in front, C_{dry}. The values for C_{dry} ranges from 0.0 for an impervious crust and best estimates of 5.5 and 9.0 based on experimental findings from the MCCI-1 separate effects SSIWCS tests and integral CCI tests, respectively [7].

To illustrate the impact of C_{dry} on the predicted accident progression, several cases were run in CORQUENCH with the Epstein/Lister water ingression model enabled with various values of C_{dry} , Figure 10. The concrete ablation ceased within 5 days for the 'Quenched' cases whereas concrete ablation was still occurring at the end of the 5 day simulated time for the 'Non-Quenched' cases. For small values of C_{dry} , the total ablation depth is quite sensitive to C_{dry} . As C_{dry} is increased, the total ablation depth became less sensitivity to C_{dry} as the melt readily quenched.

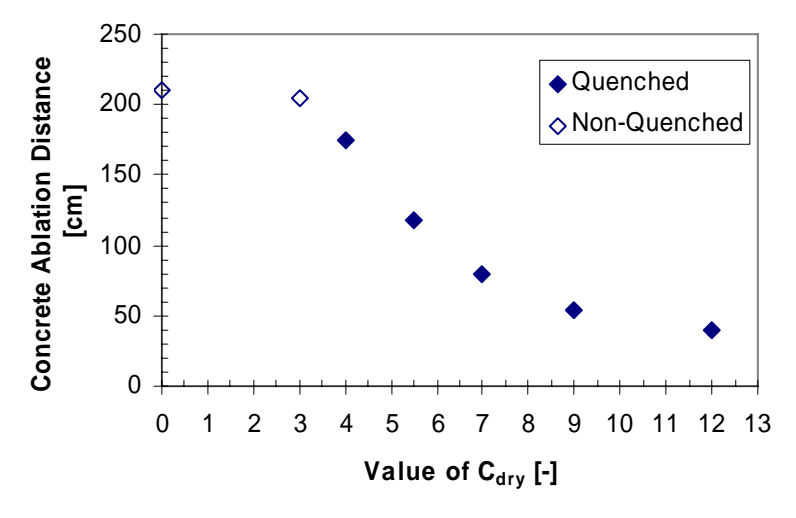


Figure 10 Water Ingression Impact on Total Ablation Depth

2.3 Melt Eruptions

Melt eruptions refer to a phenomenon where gas entrains melt from the melt pool up through channels in the top crust. The entrained melt quenches and forms a particle bed on top the crust. Melt eruptions increase the upward heat transfer and have been shown theoretically and experimentally to have a large potential to augment melt coolability. MELCOR does not allow for melt eruptions whereas CORQUENCH 3.03 currently contains four melt eruption models.

The first option is to empirically specify a melt entrainment coefficient, Ke. The melt entrainment coefficient is multiplied by the concrete decomposition gas generation rate to determine the melt ejection rate. Melt entrainment coefficients have been estimated based on post test analysis of MCCI tests and range from 0.0-2.5 x10⁻³ [14]. The Ricou-Spalding model is based on the mixing of turbulent jets and has a similar result as the purely empirical model. The melt eruption model developed by Farmer (ANL model) predicts the melt entrainment coefficient based on single phase extrusion of melt through a sinking crust, [9]. Building on the models by Farmer [9] and Tourniaire, et al. [17], a new model by Robb (UW model) was recently integrated into CORQUENCH that accounts for two-phase flow effects [10].

To show the impact of melt eruptions on melt coolability, several CORQUENCH cases we run with different melt eruption models enabled, Table 5. Including the Ricou-Spalding or ANL model yielded much less concrete ablation and melt quenching times of a little over 5 days of simulated melt-concrete contact time. The UW melt eruption model predicted rapid melt quenching. The sensitivity of melt coolability to the entrainment coefficient is demonstrated in Table 5 using values of Ke ranging from 0-2.5 x10⁻³.

Table 5 Melt Eruption Modeling in COROUENCH

Model Used	Ablation* [cm]	Quench Time [min]	Particle Bed Mass* [ton]
No eruptions ($Ke = 0.0000$) (base case)	210.0	>>7200	0
Empirical - $Ke = 0.0001$	150.0	>>7200	140
Empirical - $Ke = 0.0010$	38.6	3843	154
Empirical - $Ke = 0.0025$	29.2	614	147
Ricou-Spalding eruption model ($C = 0.08$)	51.5	>7200	167
ANL melt eruption model [10]	58.5	>7200	158
UW melt eruption model (d = 1.0 cm) [11]	27.2	176	148

^{*}At the time of melt quench or after 5 days of simulated time

2.4 Crust Anchoring and Cavity Diameter

During MCCI the top crust could anchor to the sidewalls of the reactor cavity. If the crust is able to support itself, the underlying melt could separate from the crust forming a gas layer between the melt and top crust. This has been shown to greatly impact melt coolability in laboratory scale MCCI tests [6]. However, at the plant scale the crust strength is likely not sufficient to support itself and the crust will likely remain floating on top of the melt.

Within CORQUENCH an equation has been implemented that can predict the occurrence of crust anchoring and subsequent melt separation, Eqn (2) [7]. To investigate the impact of crust anchoring on melt progression, several CORQUENCH cases were run varying cavity diameters enabling/disabling the Epstein/Lister water ingression model while keeping the crust strength fixed at 3 MPa. Water ingression, Section 2.2, allows for crusts thicker than the conduction limited case to form. A summary of the results is provided in Table 6.

TC 11 (T	<u> </u>			-
Table 6	Impact of	('riigh.	Anchoring or	n Accident	Progression
I abic 0	impact of	Clust	menoring of	1 / teclucit	1 10210331011

Concrete Ablation [cm]				
Crust	Water Initial Cavity Diameter [m]			
Anchoring	Ingression	9.34	8	7
Off	On	53	94	140
On	On	53	<u>131</u>	<u>197</u>
Off	Off	210	246	273
On	Off	210	246	273

Bold values indicate the melt quenched within 5 days <u>Underlined</u> values indicate crust anchoring occurred

$$\delta_{\text{cr,min}} = \frac{\rho_{\text{cr}} \cdot A_{\text{cr}} \cdot g}{2 \cdot C_{\text{geom}} \cdot \sigma_{\text{cr,fail}}} + \frac{1}{2} \sqrt{\left(\frac{\rho_{\text{cr}} \cdot A_{\text{cr}} \cdot g}{C_{\text{geom}} \cdot \sigma_{\text{cr,fail}}}\right)^2 + \frac{4 \cdot g \cdot (m_{\text{bed}} + m_{\text{water}})}{C_{\text{geom}} \cdot \sigma_{\text{cr,fail}}}}$$
(2)

With water ingression enabled, crust anchoring and melt separation occurred when the cavity diameter was 7 and 8 meters. Crust anchoring resulted in these cases not quenching within 5 days of simulated time. For the cases where water ingression was disabled, the crust thickness was insufficient for the crust to anchor and support itself.

In Eqn (2), $\delta_{cr,min}$ is the minimum thickness of crust necessary for crust anchoring to occur, $\sigma_{cr,fail}$ is the failure stress of the crust, ρ_{cr} is the crust density, A_{cr} is the crust surface area, g is gravity, m_{bed} and m_{water} is the mass of the particle bed and overlying water, respectively [7]. C_{geom} is a parameter which accounts for the boundary constraints and failure mode of the crust and can range from 2.53 to 8.84 [7]. Currently, the user specifies the crust strength and C_{geom} (3.0 MPa and 2.53 were used in the base case). Sample calculations for $\delta_{cr,min}$ are provided in Table 7 where ρ_{cr} is 5500 kg/m³, A_{cr} is 68.48 m², m_{bed} is 0.0 kg, and m_{water} is 66 tons (about 1 m of water).

Table 7 Minimum Crust Thickness Required for Crust Anchoring

C _{geom} [-]	σ _{cr,fail} [MPa]	$\delta_{\rm cr,min}$ [cm]
2.53	0.5	308
2.53	3.0	62
2.53	6.0	36
4.71	3.0	38
8.83	3.0	24

Given the potentially large impact of crust anchoring on melt coolability a database has been developed as part of the MACE and MCCI research programs. A database of 33 crust strength

measurements from the MACE and SSWICS test series yields crust strengths between 1-18 MPa at room temperature [8]. Three crust strength measurements from the CCI tests at elevated temperatures had strengths between 0.2-1.2 MPa [8]. Uncertainties in the crust strength and the value for C_{geom} coupled with the uncertainties in the water ingression modeling, can have a large impact on the criterion for crust anchoring, Table 7, and therefore melt coolability simulations, Table 6.

2.5 Ablation Model

MELCOR and CORQUENCH both contain a quasi-steady concrete ablation model for which all the energy deposited into the concrete goes towards concrete ablation. The quasi-steady ablation model was used by both codes in the base case calculations. CORQUENCH also contains two other more rigorous ablation models [7]. The fully developed dry out model takes into account conduction of heat into the concrete. The concrete temperature profile is initialized to the fully developed profile, ignoring the initial transient heat up of the concrete. The transient dry out model includes the initial heat up of the concrete and the possible growth and dissolution of interstitial crusts between the melt-concrete interfaces.

Table 8 summarizes the impact the three ablation models have on the accident progression simulations in CORQUENCH. All three ablation models produced similar ablation results. If the initial melt temperature was cooler an interstitial crust could form at the melt-crust interface which would decrease the initial high concrete ablation rate. Although not seen in the current simulation, this was demonstrated in a previous work [15]. The ability to capture the initial heat up transient with possible crust formation (as with the transient dryout ablation model) has aided in code validation against laboratory sized MCCI, [7], tests and could be useful in modeling the relocation of low temperature melts.

Table 8 Ablation Modeling in CORQUENCH

	Ablation Distance
Ablation Model	After 5 days [cm]
Quasi-Steady Ablation (base case)	209.5
Fully Developed Concrete Dryout	198.7
Transient Dryout	198.7

2.6 Melt Pool Configuration

MELCOR has the ability to model multiple segregated layers of melt, whereas CORQUENCH models the melt as homogeneous. As noted earlier, the pool was treated as homogeneous in the MELCOR base case settings (MIXING = -1). To investigate the impact of treating the melt as non-homogeneous, the base case was re-run in MELCOR with the mixing model enabled, (MIXING = 0). This model uses criteria to determine whether the different melt pool constituents are well mixed or stratify. Figure 8 compares the homogeneous ablation profiles to those with the mixing model enabled. Enabling mixing resulted in lower radial ablation and more aggressive axial ablation.

3.0 Summary and Recommendations

Given the differences between the codes, when similar modeling options are utilized, CORCON-Mod3 within MELCOR and the CORQUENCH code produced similar accident progression predictions. However, major differences were noted in the determination of the film boiling heat flux and melt liquidus temperature.

When models for water ingression into the top crust and melt eruptions through the top crust were included in the CORQUENCH simulations, these phenomena had a large impact on the accident progression. A previous statistical sensitivity study also demonstrated the importance of these two phenomena [16]. A basic parametric study has also shown the high potential for melt eruptions to quench the debris [17]. An increase in melt coolability due to melt eruptions and water ingression is supported by much experimental evidence, [14, 12, 6], such as the MACE M3b test where rapid quenching of half of the melt was attributed to water ingression and a 70 cm tall eruption site formed ejecting 26% of the initial melt mass [18, 6].

While melt eruptions and water ingression have a beneficial impact on melt coolability they also increase the steaming rate. A large increase in steaming rate coupled with a small containment volume requires one to consider pressurization compared to containment design pressures. The impact of the water ingression phenomenon on containment pressurization was shown in previous simulations with the MAAP 5.0.1 code [19].

For the base case set of conditions, including the crust anchoring model, using different ablation models, or causing early film boiling breakdown, did not have large impact on the CORQUENCH simulations. However, it was shown that if the cavity diameter was smaller than the relatively large sized cavity of the Zion plant and water ingression was included, crust anchoring could occur. In simulations where crust anchoring occurred, the phenomenon had a substantial negative impact on melt coolability. The impact and importance of crust anchoring agrees with a previous statistical sensitivity study [16]. Crust anchoring has been observed to occur and inhibit melt coolability in many laboratory scale MCCI tests [6].

CORCON-Mod3 within MELCOR should be updated to include optional models for water ingression into the top crust, melt eruptions, and the possibility for crust anchoring. Including these phenomena would allow for state-of-the-art predictions of the progression of an ex-vessel core melt accident. Including a transient concrete ablation model and the ability for early transition from film to nucleate boiling would help facilitate validation efforts against the MCCI experimental database. After including these advanced phenomenological models into MELCOR, code validation calculations against the MCCI experimental database should be performed. Additional MCCI simulations, coupled with containment pressurization, should be performed to investigate the impact of the increased steaming rate. Finally, an uncertainty analysis should be performed to identify key areas for further research focused on reducing overall uncertainty in accident progression predictions.

4.0 Acknowledgements

Support for this work was provided through the U.S. Nuclear Regulatory Commission Nuclear Education fellowship. Dr. Mitch Farmer of Argonne National Laboratory provided valuable guidance for the CORQUENCH simulation work.

5.0 References

- [1] Muir, J.F., "CORCON: a computer program for modeling molten fuel/concrete interactions," SAND-79-2114C, Sandia Labs., January 1980.
- [2] Blose, R.E., Gronager, A.J., J.E., Suo-Antilla, A.J., Brockmann, J.E., "SWISS: Sustained Heated Metallic Melt/Concrete Interactions with Overlying Water Pools," NUREG/CR-4727, SAND85-1546, Sandia National Lab., Albuquerque, NM, 1987.
- [3] Copus, E.R., Blose, R.E., Brockmann, J.E., Gomez, R.D., Lucero, D.A., "Core-Concrete Interactions Using Molten Steel with Zirconium on a Basaltic Basemat: The SURC-4 Experiment," NUREG/CR-4494, SAND87-2008, Sandia National Lab., Albuquerque, NM, 1989.
- [4] Bradley, D.R., Gardner, D.R., Brockmann, J.E., Griffith, R.O., "CORCON-Mod3: An Integrated Computer Model for Analysis of Molten Core-Concrete Interactions" NUREG/CR-5843, October, 1993.
- [5] Sandia National Laboratories, "MELCOR Computer Code Manuals," Version 2.1, September, Draft, NUREG/CR-6119, 2008.
- [6] Farmer, M.T., Kilskonk, D.J., Aeschlimann, R.W., "Corium Coolability Under Ex-Vessel Accident Conditions for LWRs," *Nuclear Engineering and Technology*, Vol. 41, No. 5, June 2009.
- [7] Farmer, M.T., "The CORQUENCH Code for Modeling of Ex-Vessel Corium Coolability Under Top Flooding Conditions, Code Manual Version 3.03", OECD/MCCI-2010-TR03, Draft March 2010.
- [8] S. Lomperski and M. T. Farmer, "Corium Crust Strength Measurements," *Nucl. Eng. Design*, 239, pp. 2551-2561, 2009.
- [9] Farmer, M. T., "Phenomenological Modeling of the Melt Eruption Cooling Mechanism during Molten Corium Concrete Interaction (MCCI)," <u>Proc. of ICAPP'06</u>, ANS, June 4-8, Reno, NV, USA, 2006, pp. 1296-1305.
- [10] Robb, K. R., and Corradini, M. L., "Melt Eruption Modeling for MCCI Simulations," <u>Proc. of NURETH-14</u>, ANS, September 25-30, Toronto, Canada, 2011, paper 290.
- [11] S. Lomperski and M. T. Farmer, "Experimental Evaluation of the Water Ingression Mechanism for Corium Cooling," *Nucl. Eng. Design*, 237, 905, 2007.
- [12] Farmer, M. T., Spencer, B. W., "Effects of Water Subcooling, Purity, and Pool Agitation on the Minimum Film Boiling Temperature for Metal and Oxide Surfaces," ANL/LWR/SAF 84-20, 1983.

- [13] Epstein, M.. "Dryout heat flux during penetration of water into solidifying rock," <u>J. Heat Transfer</u>, 128, 847–850, 2006.
- [14] Robb, K. R., and Corradini, M. L., "Towards Understanding Melt Eruption Phenomenon during Molten Corium Concrete Interaction," <u>Proc. of ICONE-18</u>, ASME, May 17-21 Xi'an, China, 2010, paper 30116.
- [15] Robb, K.R., "Ex-Vessel Core Melt Coolability Simulation with CORQUENCH and MELCOR," <u>Proc. of OECD-NEA MCCI Seminar 2010</u>, Cadarache, France, Nov 15-17, 2010.
- [16] Robb, K. R., Corradini, M. L., "Ex-Vessel Corium Coolability Sensitivity Study with CORQUENCH Code," Proc. of NURETH-13, Sept. 27-Oct. 2, Kanazawa, Japan, paper N13P1290, 2009.
- [17] Tourniaire, B., Seiler, J. M., Bonnet, J. M., "Experimental Study and Modeling of Liquid Ejection through Orifices by Sparging Gas," Nuclear Engineering and Design, **236**(19-21) pp. 2281-95, 2006.
- [18] Farmer, M.T., Aeschlimann, R.W., Kilsdonk, D.J., "Results of the MACE Test M3b Posttest Debris Characterization," EPRI, ACEX-TR-C33, 2001.
- [19] Paik, C.Y., Reeves, R.W., Henry, R.E., Zhou, Q., "Current Status of Molten Corium and Concrete Interaction Modeling in MAAP," <u>Proc. of OECD-NEA MCCI Seminar 2010</u>, Cadarache, France, Nov 15-17, 2010.